Oxygen transfer variation along steps of a prototype-scale stepped spillway in nappe flow regime

Author(s):
Jamali Rovesht, Tohid; Bung, Daniel B.; Archambeau, Pierre; Pirotton, Michel; Dewals, Benjamin; Erpicum, Sebastien

Publication date:
2025

Permanent link:
https://doi.org/10.3929/ethz-b-000727193

DOI: 10.3929/ethz-b-000727193

Oxygen transfer variation along steps of a prototype-scale stepped spillway in nappe flow regime

T. Jamali[1], D. Bung[2], P. Archambeau[1], M. Pirotton[1], B. Dewals[1], S. Erpicum[1]
[1]Liege University, Liege, Belgium
[2] FH Aachen University, Aachen, Germany
E-mail : Tohid.Jamalirovesht@uliege.be

***Abstract**. Based on long-term data, oxygen levels have decreased in temperate natural lakes because of thermal stratification and eutrophication. Similar conditions can be observed in newly filled reservoirs, with consequences on the environment. Air-water flows taking place on hydraulic structures are helpful to increase the dissolved oxygen concentration. However, due to the complex nature of the air-water flows and scale effects distorting results from scale physical models, investigations are still needed to better characterize the effect of flow past hydraulic structures on dissolved oxygen concentration. In this paper, laboratory experiments conducted at the Engineering hydraulics laboratory (HECE) at Liege University on a prototype scale 15° stepped spillway made of 6 steps 50 cm high and operated in nappe flow conditions are presented. The objective of these tests was to document the oxygen transfer profile along different steps by means of direct dissolved oxygen concentration measures. The concentration of dissolved oxygen was continuously measured using optical DO sensors and validated by Winkler tests. The optical sensors yield reliable results when not placed in bubbly flows or under jet impact. The results showed that, on individual steps, aeration efficiency decreases with an increase in flow rate. The filling of the cavity below the nappe accelerates this reduction. Aeration efficiency from the upstream edge to the cavity is slightly higher than from upstream edge to downstream edge of a step when the cavity is not full of water.*

***Keywords:** Oxygen transfer, Stepped spillway, Air-water flows, Prototype-scale model, Optical DO sensors*

1. Introduction

Dissolved oxygen (DO) indicates the amount of oxygen (O_2) freely dissolved in water. The survival of most aquatic plants and animals depends on DO concentration (Schindler 2017) with negative effects when values are too low or too high. Furthermore, the DO concentration influences nutrient biogeochemistry, greenhouse gas emissions, drinking water quality, and thus human health (North et al. 2014; Fernández et al. 2014; Michalak et al. 2013; Harke et al. 2016). As highlighted by Jane et al. (2021), there has been a decrease in DO concentrations in both surface and deep waters of natural lakes from 1980 to 2017, with reductions of 0.45 mg/l and 0.42 mg/l, respectively. This decline is associated with thermal stratification and a reduction in solubility resulting from an increase in temperature. Also, the excessive growth of bacteria induced by the eutrophication limits the amount of dissolved oxygen in stagnant waters.

Similar conditions can be observed in man-made reservoirs particularly within the initial years after impounding such as at Petit Saut dam in France (Gosse and Gregoire 1997) and Nam Theun 2 Hydropower dam in Laos (Descloux et al. 2015). The stratification phenomenon creates layers in reservoir volume, hindering the proper mixing of water. This leads to a decrease in oxygen levels in the reservoir's lower layers (hypoxia). Additionally, the reduction of oxygen can increase the release of phosphorus (P) bound to sediment particles, which accelerates eutrophication, blooms of algae, phytoplankton and ultimately results in further oxygen depletion (Friedl and Wüest 2002; Kunz et al. 2011; Nurnberg 1984). Various management strategies can be employed to uphold good ecological conditions and ensure a sufficient DO in water released downstream from reservoirs such as turbine air injection, surface water

pumps, oxygen injection and aeration on hydraulic structures such as stepped spillways, plunging pool and free jets. Among these methods, hydraulic structures are preferred since other alternatives typically consume energy (Winton et al. 2019; Beutel and Horne 1999). Moreover, flow aeration at hydraulic structures enhances their safety by addressing potential issues such as cavitation erosion (Russell and Sheehan 1974; Falvey 1990), and excessive energy levels (Chanson and Lee 1997; Hoque and Aoki 2005).

Due to the large size of such structures and the inability to control flow conditions in the field, most studies take place in laboratory setups under controlled conditions and at a reduced scale. Applying Froude similarity in free surface flows does not adequately scale viscous and surface tension forces, but these forces play a key role in air-water interaction. Therefore, air-water flows, and gas transfer estimation can be distorted by so called scale effects (Pfister and Chanson 2014; Chanson and Gonzalez 2005; Felder and Chanson 2017).

Oxygen transfer through the air – water interface is driven by the concentration gradient between the two phases. In practical contexts, this process is typically quantified using the mass transfer equation, as described by Cussler (1997).

$$C_{P,T,S} = C_{Sa\ P,T,S} - (C_{Sa\ P,T,S} - C_0) * e^{-k_L * a * t} \quad (1)$$

where $C_{P,T,S}$ is the oxygen concentration in the liquid phase at local pressure P, temperature T and salinity S, $C_{Sa\ P,T,S}$ is the saturation concentration at local conditions, C_0 is the initial concentration, k_L is the mass transfer coefficient or mass transfer velocity (in m/s) of the liquid phase, $a = A/V$ is the specific air water interface (in m^2/m^3) with A the total interface available for mass transfer in the water volume V, and t is time.

To compare aeration performance with different local conditions, $C_{P,T,S}$ can be normalized to a standard temperature of 20 ℃, pressure of 1013.25 hPa and considering salinity effect with a correction factor S_c (U.S. Geological Survey, 2020), such as:

$$C_{20} = C_{P,T,S} * \frac{C_{Sa,20}}{C_{Sa,T}} * \frac{1013.25}{P} * S_c \quad (2)$$

Also, the oxygen transfer can be evaluated by other values such as the deficit ratio r_T or the aeration efficiency E, which are defined as

$$r_T = [(C_{Sa} - C_u) / (C_{Sa} - C_d)] \quad (3)$$

$$E_T = 1 - 1/r_T = [(C_d - C_u) / (C_{Sa} - C_u)] \quad (4)$$

where C_d and C_u are the downstream and upstream DO concentration, respectively. Hinze (1995) and Azbel (1981) suggested temperature correction factor for normalization of E_T to a standard temperature of 20 ℃ as follows

$$1 - E_{20} = (1 - E_T)^{1/f} \quad (5)$$

$$f = 1 + 0.02103(T - 20) + 8.261 * 10^{-5} (T - 20)^2 \quad (6)$$

To predict the aeration efficiency E_{20} in a stepped spillway, known for flow aeration and energy dissipation, several empirical equations based on experimental results have been proposed. For instance, Baylar et al. (2007) considered chute height H of 1.25 and 2.5 m, step height h_s of 0.05, 0.1, and 0.15 m, chute slope θ ranging from 14.48° to 50°, and unit discharge q from 0.0167 to 0.1667 m²/s. They found that the aeration efficiency in nappe flow regime can be evaluated as:

$$E_{20} = 1\text{-}\left[exp\left(1 - 0.265(sin\theta)^{-2.661}\left(\frac{h_c}{h_s}\right)^{0.007} {L_a}^{-2.057}\right)\right]^{-1.575} \quad (7)$$

with h_c, the critical flow depth, and $L_a = \frac{H}{\sin\theta} - 6.834{h_s}^{0.749} q^{0.205} (\cos\theta)^{0.915}$

Essery et al. (1978), considering stepped spillways with chute height H of 1 and 2 m, step height h_s ranging from 0.025 to 0.5 m, chute slope θ between 11.3° and 45°, and unit discharge q from 0.0116 to 0.1447 m²/s, proposed the following equation for aeration efficiency, independently of the flow regime:

$$E_{20} = 1\text{-}\left[exp\left(-\frac{H}{\sqrt{g h_s}}\left[0.427 - 0.310\, ln\left(\frac{h_c}{h_s}\right)\right]\right)\right] \quad (8)$$

Khdhiri et al. (2014), based on available literature data and their own experimental results, proposed an equation that relates to Reynolds number Re, chute slope θ , number of steps n, and chute height H. Their study covered unit discharge q from 0.002 to 0.0083 m²/s, chute slope θ between 26.56° and 35.53°, step height h_s ranging from 0.05 to 0.1 m, and chute height H of 0.25 and 0.5 m.

$$E_{20} = 0.331\, Re^{-0.048}\, n^{0.687}\left(\frac{h_c}{H}\right)^{0.169} (tan\,\theta)^{0.234} \quad (9)$$

According to the literature, prior studies have largely focused on the overall aeration efficiency of stepped spillways, while there are limited results about oxygen transfer on a single step. However, since one must select a consistent measurement position on the steps when characterizing the aeration taking place over a stepped spillway reach, and since flow conditions on the steps of stepped spillway are complex, selecting the appropriate location might be challenging. In order to characterize the influence of DO measurement position and to quantify oxygen transfer on a single step, tests have been performed to measure DO concentration at various locations on two different steps of a prototype-scale stepped spillway in nappe flow conditions.

2. Experimental facility and instrumentation

The experiments were conducted at the HECE Laboratory, University of Liege, on a prototype-scale stepped spillway (Fig. 1) with six identical steps 0.5 m high, 1.87 m long (resulting in a 15° slope), and 0.2 m wide, operating in the nappe flow regime. The model represented a segment of a 157-meter-wide aerating weir constructed downstream of Lom Pangar dam in Cameroon, designed and built to enhance DO concentration in the Lom River (Erpicum et al. 2016, Felder et al, 2019). Steps are numbered from I to VI from upstream to downstream (Fig. 1)

The vertical faces of the steps and the sidewalls were made of smooth plastic plates to limit side friction effects; PVC was used except on the left sidewall for which Perspex was used to ease flow visualization. The bottom of the steps was constructed from random rubble masonry, as in the prototype. Water was pumped from an underground reservoir with a capacity of 400 m³ to an upstream header tank, 1 by 1 by 3 m (in length, width, and height). A contraction smoothly directed the flow into the experimental flume section via a 1.01 m long broad-crested weir.

The flow rate was measured using a Siemens MAG 5100 electromagnetic flow meter installed on the 0.15 m diameter supply pipe. DO concentrations and temperature were measured by eight Hamilton VisiWater DO P Arc 150 FC10 optical sensors, numbered from 1 to 8, with an accuracy of ±0.4 ppm, ± 5 % at 25 °C. These sensors operate on the principle of luminescence quenching and sample at a frequency of 0.33 Hz. The signal was collected by an acquisition box which was designed at the HECE lab. The local atmospheric pressure and water conductivity were measured by Chacon weather station and Extech EC400 Conductivity/TDS/Salinity meter (±2 % FS), respectively.

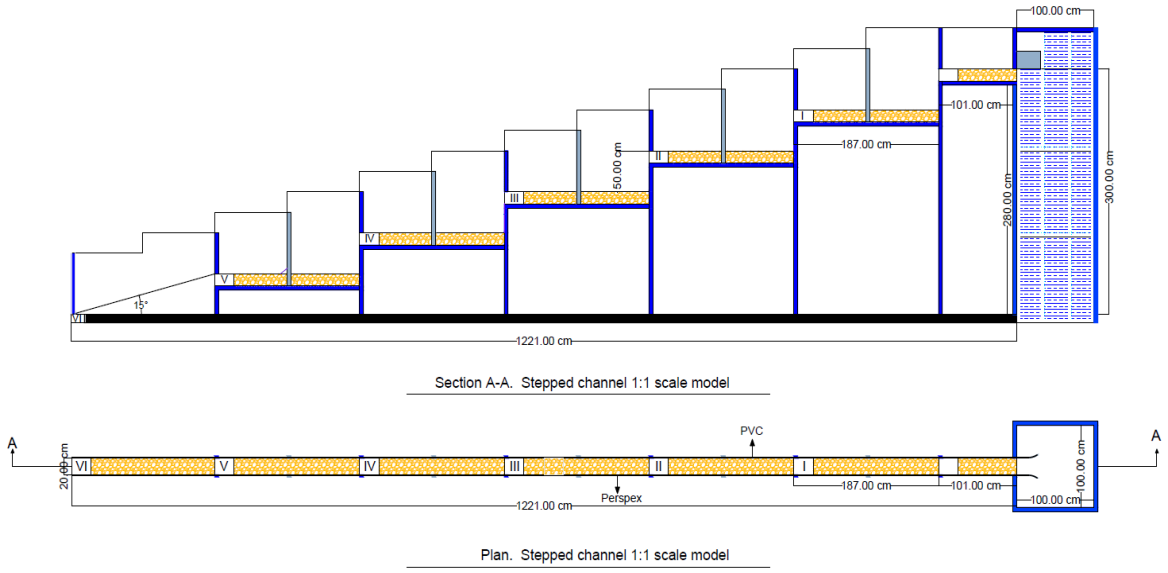

Figure 1. Sketch of the prototype-scale model with main dimensions and step numbers.

3. Methodology

Tests were carried out with unit discharges ranging from 0.2 to 0.6 m²/s. Consequently, Reynolds number $Re = q/\nu$ varied between $1.9\ 10^5$ and $5.8\ 10^5$. For the tested discharge range, one of the key features of the flow on a step is the presence of an air cavity below the free-falling jet (Fig. 2 and Fig. 3). This cavity experiences a fluctuating free surface level that increases with discharge. The cavity completely fills with water when discharge exceeds a threshold whose value varies depending on step location along the spillway. Tests were performed on steps I and IV since they experienced different cavity conditions for the tested discharge range (Fig. 2). Jet length, flow depth within the cavities, and flow depth after jet impact were considered to determine the position of the optical sensors on the steps. As shown in Figure 2, nine different positions labelled A to I were considered along each step, at channel centerline.

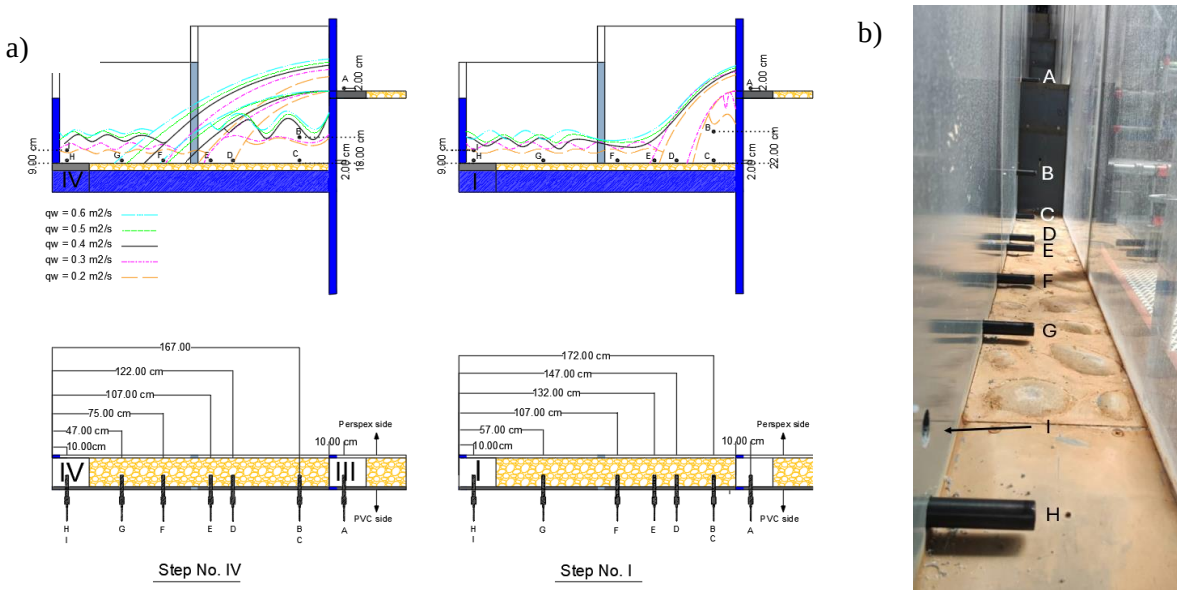

Figure 2. a) Sketch of flow trajectories at various flow rates on steps I and IV and positions from A to I of optical sensors - b) Positions from A to I of optical sensors on step IV

To supply water to the model with a minimal DO concentration, 100 g/m³ of sodium sulfite (Na_2SO_3) were added to the 400 m³ tank and mixed with a submerged pump 12 hours before conducting a test. 1 g/m³ of cobalt chloride ($CoCl_2$) had been added once as a catalyst. To prevent chemical excess, which can affect the reaeration process during testing, the DO concentration in the reservoir wasn't reduced below approximately 1 mg/l.

During a test, flow rate was increased from 0.2 or 0.4 to 0.6 m²/s with a step of 0.1 m²/s. Each discharge was kept constant for 6 min and data was recorded continuously. The upstream oxygen concentration slowly increased as oxygenated water from the model mixed with the residual deoxygenated water in the reservoir. Test duration was such that DO concentration did not reach the saturation level. Water conductivity, temperature, and local pressure were noted to normalize the data to standard conditions. Also, during selected tests, Winkler tests were performed on water samples collected along the jet trajectory before impact for comparison and validation of the data from optical sensors.

To improve results reliability, six tests were conducted for each step, varying the sensors' position (Table 1). Three of these configurations included positions A to H, while the remaining configurations involved positions A to I, without position D.

Table 1. Tests conditions

Test No	Water temperature (℃)		Atmospheric pressure (hPa)		Conductivity ($\mu S/cm$)		Unit discharge (m²/s)	Time (min)	Winkler test		Position of the optical sensors on steps I and IV
	Step No. I	Step No. IV	Step No. I	Step No. IV	Step No. I	Step No. IV			Step No. I	Step No. IV	
Test 1	20	17.3	984	990	1060	-	0.2	6	★		
							0.3	6			
							0.4	6			
							0.5	6			
							0.6	6			
Test 2	20.5	17.5	989	991	1235	-	0.2	6			
							0.3	6	★		
							0.4	6			
							0.5	6	★		
							0.6	6			
Test 3	19	17.75	988	980	1285	-	0.2	6			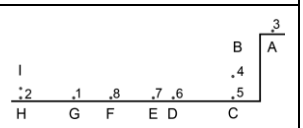
							0.3	6			
							0.4	6	★		
							0.5	6			
							0.6	6	★		
Test 4	21	17.75	983	992	1330	-	0.4	6	★		
							0.5	6			
							0.6	6	★		
Test 5	19	18	988	988	1480	-	0.4	6		★	
							0.5	6	★		
							0.6	6			
Test 6	19	18.2	984	984	1570	960	0.4	6			
							0.5	6		★	
							0.6	6	★		

4. Results

4.1 Flow observations

Visual observations confirmed that the flow regime is nappe flow for all the tested discharges. As the flow rate increased, jet length, flow depth after jet impact, and water depth in the cavity also increased, with greater instability of the flow and strong splashing. Step I cavity was fully filled with water 50% of the time at a flow rate of 0.3 m²/s. For flow rates above 0.3 m²/s, this cavity was continuously filled and the cavity of step II started to be randomly filled with water, while the other steps' cavities remained partly filled but with varying water depth (see Figure 3).

Figure 3. Flow conditions a) over the whole model at flow rate of 0.2 m²/s, b) at steps I and II at flow rate of 0.6 m²/s, and c) in the cavity of step IV at flow rate of 0.4 m²/s.

4.2 DO concentration and aeration efficiency

Average values of DO concentration measured by the optical sensors have been calculated for each flow rate and position (Fig. 4). The results show a good agreement between the Winkler tests and optical sensor data, especially at locations C and D, which were close to the Winkler tests sampling area.

DO concentration measured values were generally consistent from test to test despite slightly different initial conditions, except at step edges (locations A, H and I), in particular on step IV, such as highlighted by the red boxes on figure 4. The large variation of results at these locations can be attributed to the limited flow depth, high flow velocity, and high air concentration, which caused the sensor to be randomly out of the water or be in contact with air bubbles. As the flow rate increased, this discrepancy decreased.

When measurements are consistent, lowest DO concentration is logically measured upstream of the step (location A). Along a step, DO concentration variation is small, specifically for higher discharges. For small discharges, maximum DO concentration is usually measured in the cavity (locations B and C) and minimum at jet impact area (location D on step I and F on step IV).

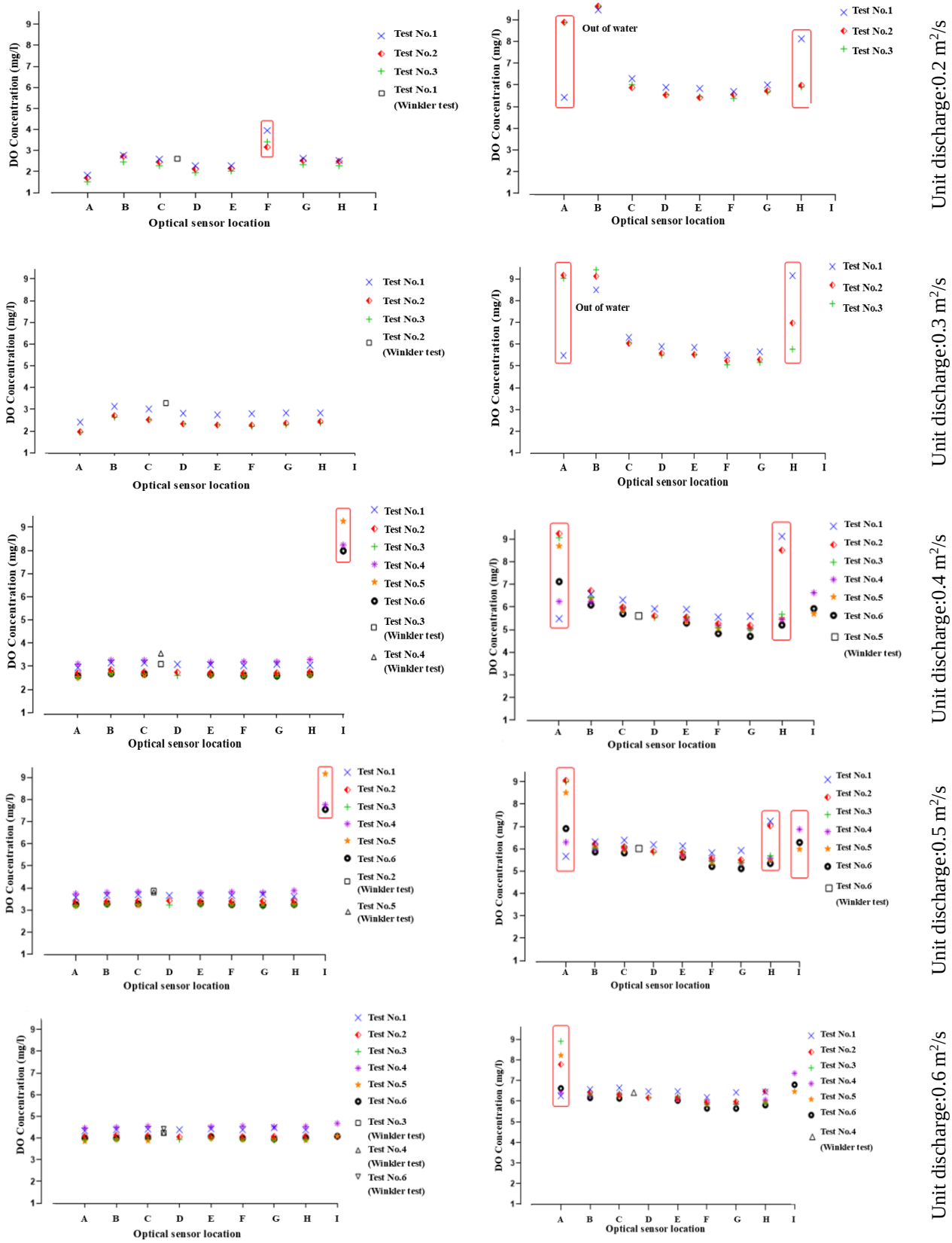

Figure 4. Average DO concentrations measured by optical sensors and Winkler tests results at various unit discharges and locations on step I (left) and IV (right).

Figures 5 and 6 display the average and variation range of aeration efficiency at 20 °C (E20) on steps I and IV, calculated from A to H (upstream of the step to the end of the step) and from A to C (upstream of the step to the cavity). On step IV, only the results from tests 1 and 4 have been considered due to overestimated values of DO concentration at locations A and H for the other tests.

On both steps, aeration efficiency decreases with an increasing flow rate. On step I, the complete filling of the cavity (discharge higher than 0.3 m²/s) corresponds to a strong reduction in the slope of aeration efficiency decrease. On a single step, a partly filled cavity below the jet significantly improves aeration efficiency compared to a cavity constantly drowned. Overall, aeration efficiency from upstream of the step to the cavity is higher than from upstream of the step to the end of the step, with a difference reaching 2.6 % on step I and the smallest discharge, i.e. when the cavity is less filled with water. When the cavity is drowned, aeration efficiency variation is less than 1%, i.e. much less than measurement uncertainty.

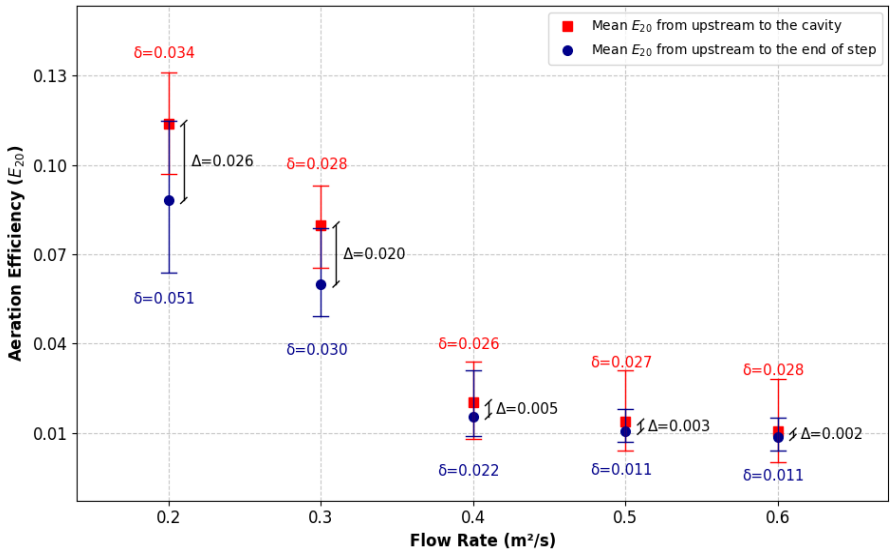

Figure 5. Averaged aeration efficiency at 20 °C (E_{20}) and measurements variation depending on flow rate on step I.

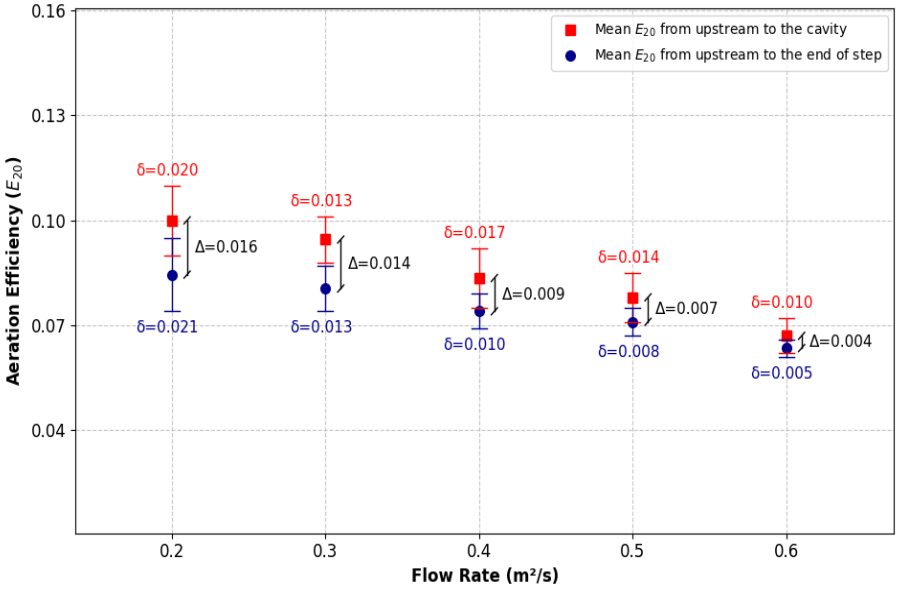

Figure 6. Averaged aeration efficiency at 20 °C (E_{20}) and measurements variation depending on flow rate on step IV.

5. Conclusion

In this study, the oxygen transfer along different steps of a prototype-scale stepped spillway operating in nappe flow regime was carefully analyzed. The results show that

- Optical sensors data and Winkler test results are in good agreement, but the presence of a lot of air bubbles may strongly affect DO sensors.
- Global aeration efficiency on a single step decreases with increasing flow rate; the presence of an air cavity below the jet at step entrance greatly improves aeration.

On a single step, oxygen transfer is lower from step upstream end to step downstream end than from step upstream end to the cavity when the cavity exists, i.e., is not constantly filled with water. When the cavity is drowned, aeration efficiency is not significantly different from step upstream end to step downstream end than from step upstream end to the cavity.

If one would characterize the aeration taking place over a stepped spillway reach in nappe flow conditions, and consequently needs to select a consistent measurement position on the steps, placing the sensors in the corner below the jet is recommended since this location is away from highly bubbly flow and jet impact.

6. Acknowledgments

The results were gained in the framework of a joint research project funded by the Deutsche Forschungs-gemeinschaft (DFG, German Research Foundation) – project no. 511289281 – and the Fonds National de la Recherche Scientifique (F.R.S.-FNRS, Belgian Research Fund) - project no. TW004.23F – PDR-WEAVE-DFG.

7. References

Azbel, D. (1981). “Two-phase flows in chemical engineering”. Cambridge, England: Cambridge University Press.

Baylar, A., Bagatur, T., & Emiroglu, M.E. (2007). “Prediction of oxygen content of nappe, transition and skimming flow regimes in stepped-channel chutes”. Environmental Engineering and Science. 6(2), 201–208, https://doi:10.1139/s06-048.

Beutel, M. W., and Horne, A. J. (1999). “A Review of the Effects of Hypolimnetic Oxygenation on Lake and Reservoir Water Quality”. Lake and Reservoir Management, 15(4), 285–297, https://doi.org/10.1080/07438149909354124.

Chanson, H., and Lee, J. F. (1997). “Plunging jet characteristics of plunging breakers”. Coastal Engineering, https://doi.org/10.1016/S0378-3839(96)00056-7.

Chanson, H., and Gonzalez, C. A. (2005).” Physical modelling and scale effects of air-water flows on stepped spillways. Journal of Zhejiang University - Science A: Applied Physics & Engineering, 6A (3). https://doi: 10.1007/BF02872325.

Cussler, E.L., Diffusion - Mass transfer in fluid systems; Cambridge University Press: Cambridge, 1997, ISBN 0 521.

Descloux,S., Chanudet, V., Taquet, B., Rode, W., Guédant, P., Serça, D., Deshmukh, C., & Guerin, F. (2015). “Efficiency of the Nam Theun 2 hydraulic structures on water aeration and methane degassing”. Hydroécol. Appl. Published online on 25 March 2015, https://doi: 10.1051/hydro/2015002.

Essery, I.T.S., Tebbutt, T.H.Y., & Rajaratnam, S.K. (1978). “Design of spillways for re-aeration of polluted waters.” Construction Industry Research and Information Association, Report 72, London, UK.

Erpicum, S., Lodomez, M., Savatier, J., Archambeau, P., Dewals, B., & Pirotton, M. (2016). “Physical modeling of an aerating stepped spillway”. 6th International Symposium on Hydraulic Structures Portland, Oregon, USA, doi:10.15142/T3680628160853.

Falvey, H. T. (1990). “Cavitation in chutes and spillways”. Denver, CO, USA: US Department of the Interior, Bureau of Reclamation.

Fernández, J. E., Peeters, F., & Hofmann, H. (2014). “Importance of the autumn overturn and anoxic conditions in the hypolimnion for the annual methane emissions from a temperate lake”. Environmental Science and Technology 48(13), 7297–7304, https://doi.org/10.1021/es4056164.

Felder, S., Chanson, H. (2017).” Scale effects in microscopic air-water flow properties in high-velocity free-surface flows”. Experimental Thermal and Fluid Science, 83, 19-36, https://doi.org/10.1016/j.expthermflusci.2016.12.009.

Felder, S., Geuzaine, M., Dewals, B., & Erpicum, S. (2019).” Nappe flows on a stepped chute with prototype-scale steps height: Observations of flow patterns, air-water flow properties, energy dissipation and dissolved oxygen”. Journal of Hydro-environment Research, 27, 1–19, doi.org/10.1016/j.jher.2019.07.004.

Friedl, G., and Wüest, A. (2002). “Disrupting biogeochemical cycles – Consequences of damming”, Aquatic Sciences, 64, 55–65, https://doi.org/10.1007/s00027-002-8054-0.Gosse, Ph., and Grégoire, A. (1997). “Artificial re-oxygenation of the Sinnamary, downstream of Petit-Saut dam (French Guiana).” Hydroécol. Appl. 9(1-2), 23-56. (In French)

Harke, M. J., Steffen, M. M., Gobler, C. J., Otten, T. G., Wilhelm, S. W., Wood, S. A., & Paerl, H. W. (2016). “A review of the global ecology, genomics, and biogeography of the toxic cyanobacterium, Microcystis spp”. Harmful Algae, 54, 4–20, https://doi.org/10.1016/j.hal.2015.12.007.

Hinze, J.O. (1955). “Fundamentals of the hydrodynamic mechanism of splitting in dispersion processes”. *AIChE Journal*, 1(3), 289–295, doi:10.1002/aic.690010303. Hoque, A., and Aoki, S. (2005). “A quantitative analysis of energy dissipation among three typical air entrainments”. Env. Fluid Mech., 5, 325 – 340, https://doi:10.1007/s10652-005-3258-1.

Jane, S.F., Hansen, G.J.A., Kraemer, B.M. et al. (2021).” Widespread deoxygenation of temperate lakes”. Nature, 594, https://doi.org/10.1038/s41586-021-03550-y.

Khdhiri, H., Potier, O., & Pierre, J. (2014). “Aeration efficiency over stepped cascades: Better predictions from flow regimes”, Water Research, 55, 194-202, https://doi.org/10.1016/j.watres.2014.02.022.

Kunz, M. J., Wüest, A.,Wehrli, B., Landert, J., & Senn, D. B. (2011). “Impact of a large tropical reservoir on riverine transport of sediment, carbon, and nutrients to downstream wetlands”, Water Resources Research, 47, 1–16, https://doi.org/10.1029/2011WR010996.

Michalak, A. M. Anderson, A. J., Beletsky, D., & Zagorski, M. A. (2013). “Record-setting algal bloom in Lake Erie caused by agricultural and meteorological trends consistent with expected future conditions”. Proceedings of the National Academy of Sciences 110(16), 6448–6452, https://doi.org/10.1073/pnas.121600611

North, R. P., North, R. L., Livingstone, D. M., Köster, O. & Kipfer, R. (2014). “Long-term changes in hypoxia and soluble reactive phosphorus in the hypolimnion of a large temperate lake: consequences of a climate regime shift”. Global Change Biology. 20, 811–823, https://doi: 10.1111/gcb.12371.

Nurnberg, G. K. (1984). “The prediction of internal phosphorus load in lakes with anoxic hypolimnia” Limnology and Oceanography, 29, 111–124, https://doi.org/10.1016/j.scr.2014.10.005.

Pfister, M., and Chanson, H. (2014). “Two-phase air-water flows: Scale effects in physical modeling”. Hydrodynamics, 26(2), 291-298, https://doi.org/10.1016/S1001-6058(14)60032-9.

Russell, S. O., and Sheehan, G. J. (1974). “Effect of entrained air on cavitation damage”. Canadian Journal of Civil Engineering, 1, 97 – 107, https://doi:10.1139/l74-008.

Schindler, D. (2017). “Warmer climate squeezes aquatic predators out of their preferred habitat”. Proceedings of the National Academy of Sciences. USA, 114(37), 9764–9765, https://doi.org/10.1073/pnas.171281811.

Winton, R.S.; Calamita, E.; Wehrli, B. (2019). “Reviews and syntheses: Dams, water quality and tropical reservoir stratification”, Biogeosciences 16(8), 1657-1671, https://doi 10.5194/bg-16-1657-2019.

U.S. Geological Survey. (2020). “Chapter A6.2. Dissolved oxygen”. In Techniques and Methods, Book 9: Handbooks for Water-Resources Investigations, https://doi.org/10.3133/tm9a6.2.